Primljen / Received: 26.4.2024.
Ispravljen / Corrected: 13.8.2024.
Prihvaćen / Accepted: 2.9.2024.
Dostupno online / Available online: 10.10.2024.

Numerical analysis on wind-induced vibration response of long-span transmission tower-line system

Authors:

[1]Xianxin Li, MSc. CE
52026030@qq.com

[2]Binghao Ding, MSc. CE
dingbinghao-heny@powerchina.cn

[1]Daokun Qi, MCE
qidaokun@126.com

[2]Kaixin Zhang, MSc. CE
zhangkaixin-heny@powerchina.cn
Corresponding author

[2]Miaomiao Wang, MSc. CE
wangmiaomiao-heny@powerchina.cn

[1]Henan State Network Economic and Technological Research Institute, China
[2]PowerChina Henan - Electric Power Research and Design Institute

Research Paper

Xianxin Li, Binghao Ding, Daokun Qi, Kaixin Zhang, Miaomiao Wang

Numerical analysis on wind-induced vibration response of long-span transmission tower-line system

Based on the engineering background related to ±800 kV ultra-high voltage (UHV) transmission lines spanning the Yellow River, finite element models were developed for single-tower and transmission tower-line systems, with their wind-induced responses under wind loads were simulated and analysed. In addition, the coupling effect in a large-span transmission tower line system was investigated. The results showed that the natural vibration frequency of the tower-line system was slightly lower than that of a single tower and that the torsional natural frequency was the most significantly reduced. The transmission tower-line system has a maximum displacement of 1.92 times that of a single tower when the wind angle is 0°. The maximum axial force and stress in the tower-line system are 1.6 times and 1.37 times higher than those in a single tower. The interaction between the tower and wires significantly affects the wind-induced response of the tower body. Hence, considering the dynamic coupling effect of the tower-line transmission system is important when designing a tower.

Key words:
tower-line system, long span, vibration response, coupling effect, finite element model

Prethodno priopćenje

Xianxin Li, Binghao Ding, Daokun Qi, Kaixin Zhang, Miaomiao Wang

Numerička analiza titrajnog odziva dalekovoda velikog raspona prijenosnih vodova izazvanog vjetrom

Na temelju inženjerskih spoznaja o dalekovodima ultravisokog napona ±800 kV koji se protežu preko rijeke Huang razvijeni su modeli konačnih elemenata za pojedinačni stup i dalekovod te su simulirani i analizirani njihovi odzivi uslijed pobude vjetrom. Ispitan je i učinak međudjelovanja stupa i voda u dalekovodu velikog raspona prijenosnih vodova. Na temelju rezultata utvrđeno je da je vlastita frekvencija dalekovoda bila nešto niža od one pojedinačnog stupa, a torzijska vlastita frekvencija bila je najviše smanjena. Najveći pomak dalekovoda je za 1,92 puta veći od pomaka jednog stupa pri upadnome kutu vjetra od 0°. Najveća uzdužna sila i naprezanje u dalekovodu su 1,6 puta i 1,37 puta veći od onih u jednome stupu. Međudjelovanje između stupa i vodova znatno utječe na odziv stupa izazvanog vjetrom. Zato je pri projektiranju stupa važno uzeti u obzir učinak dinamičkog međudjelovanja stupa i voda u sustavu dalekovoda.

Ključne riječi:
dalekovod, veliki raspon, titrajni odziv, učinak međudjelovanja, model konačnih elemenata

1. Introduction

Owing to their advantages of low transmission losses and minimal land occupation, ultra-high voltage (UHV) DC transmission lines are widely used for long-distance and high-capacity power transmission. As tall, flexible structures, UHV transmission towers are prone to experiencing significant wind-induced vibrations, which directly impact the overall safety of transmission lines. Studies have demonstrated that wind load is a significant factor contributing to the collapse of transmission towers [1]. Moreover, the geometric nonlinearity of transmission lines significantly impacts the wind-induced responses of tower-line systems. Extensive research has been conducted by scholars both domestically and internationally. Ozono and Maeda [2] simplified wires into springs at high frequencies and multiple particles at low frequencies to investigate the dynamic characteristics of the transmission tower-line system in the plane. Albermani and Kitipornchai [3] proposed a nonlinear analysis theory to determine the limit response of transmission tower structures. Yasui et al. [4] adopted a time-domain analysis method to comparatively analyse the dynamic characteristics of self-supporting and guyed tower-line systems under wind loads. Geng et al. [5] derived a simplified dynamic equation for a two-tower and three-wire system and verified the validity of the approximate theory through finite element analysis. Guo et al. [6] developed a finite element model of a large-span tower-line system and analysed its wind vibration response in combination with wind tunnel testing of an aeroelastic model. Yu and Zhang [7] established a finite element model to study the dynamic characteristics of a tower line system. They found that the coupling effect on the out-of-plane vibration of tower-line systems was greater than that on the in-plane vibration. Zhang et al. [8, 9] developed a finite element model to investigate the impact of wind direction and cross-arm width on the wind-induced response characteristics of both the tower and cross-arms. Zhang et al. [10] developed a finite element model of a tower-line system consisting of three towers and two lines to study the impact of the tower-line system parameters on the modal characteristics. They found that the frequency of the transmission tower significantly increased with a longer total span length but was only slightly affected by changes in the front-rear span ratio and height difference angle. Zhu et al. [11] and Wang et al. [12] investigated the impact of different wind angles on the wind-induced response of transmission towers using finite element modelling or aeroelastic model wind tunnel tests. Lou et al. [13] and Deng et al. [14] conducted wind tunnel tests to analyse the wind vibration coefficients of transmission towers under normal and typhoon wind fields. The results indicated that the high turbulence characteristics of the typhoon wind field resulted in a larger wind vibration coefficient for the tower compared with those under a normal wind field. Yang et al. [15] used the frequency-domain analysis method to study the wind-induced vibration response of long cross-arm transmission towers and reported that considering the torsional static wind load effectively improves the guarantee rate of diagonal materials under the condition of slightly increasing the axial force of the main material.

Previous studies predominantly focused on examining the dynamic responses of towers and conductors under various wind load conditions. In China, relevant regulations treat transmission towers and conductors as separate entities, independently calculating their respective wind loads. However, relatively limited research has explored the influence of tower-line coupling effects on the wind-induced responses of towers. Based on the ±800 kV UHV transmission tower across the Yellow River, we employed the linear filtering method to simulate the pulsing wind load and establish Ansys finite element models of single-tower and tower-line systems. A numerical simulation was used to analyse the wind-induced response of a single tower and tower-line system under a wind load to investigate the impact of the tower-line coupling effect on the wind-induced response of transmission towers.

2. Finite element model

The ±800 kV UHV Yellow River long-span transmission project is key to the Hami-Zhengzhou ±800 kV transmission project. The Yellow River consists of five towers designated as N1–N5. Among these, N1 and N5 served as tension towers, whereas the remaining three were tangent towers. The transmission towers had heights of 39 m, 100 m, 136 m, 136 m, and 48 m, with spans of 450 m, 1200 m, 1350 m, and 900 m. The single-line diagrams of the towers are shown in Fig. 1.

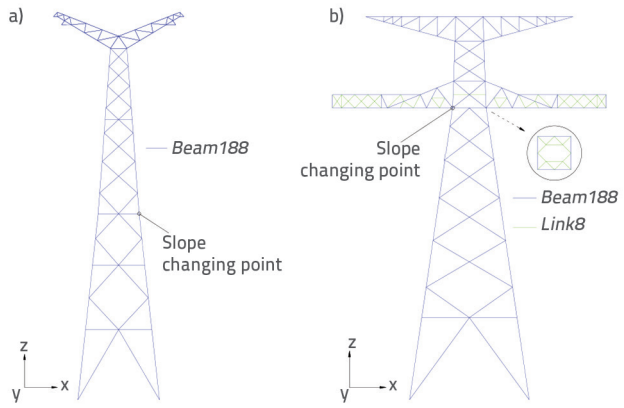

Figure 1. Tangent crossing tower (N2, N3, N4) and tension tower (N1, N5): a) Tangent crossing tower; b) Tension tower

2.1. Single tower model

The entire tangent-crossing tower was simulated using Beam188 elements. The main members of the tension tower were represented by Beam188 elements, whereas other bars, such as the auxiliary bars of the tower body and the bars in the

diaphragm, were modelled by *Link8* elements if there were no sub-nodes. Otherwise, *Beam188* elements were used for the modelling.

2.2. Tower-line system model

Transmission conductors are flexible components with low stiffness and are typically classified as suspension-cable structures. This type of structure is characterised by low natural frequency, low stiffness, ease of geometric deformation, and high nonlinearity.

To establish a finite element model of a suspension cable structure, a shape-finding analysis of the suspension cable is necessary to determine its initial shape. This study adopted the catenary method and assumed that the deadweight of the suspension cable structure was uniformly distributed along its curve, enabling a shape-finding analysis for transmission conductors. The transmission line parameters are listed in Table 1.

Link10 elements, which could only bear tension, were selected to model the wires. The finite element model of the tower line system, which comprises five towers and four lines, is illustrated in Figure 2.

Table 1. Mechanical parameters of the transmission lines

Parameter	Conductor	Ground wire
Type	JLHA1/EST-900/240	OPGW-300
Cross-sectional area [mm2]	1142.48	299.6
Diameter [mm]	44.02	22.9
Linear density [kg/m]	4.6815	2.205
Calculated breaking force [kN]	620.8	432.7
Maximum design tension [kN]	163.8	94.6
Linear expansion coefficient [1/°C]	$1.75 \cdot 10^{-5}$	$1.20 \cdot 10^{-5}$
Elastic modulus [MPa]	83190	170100

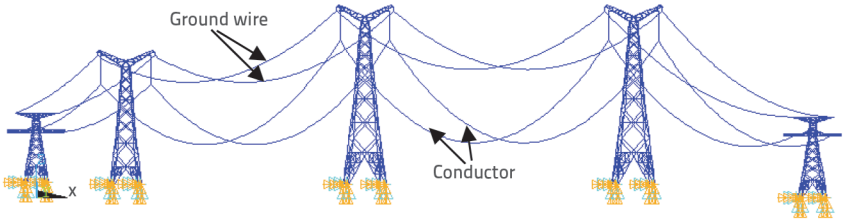

Figure 2. Finite element model of transmission tower-line system. Note: x-direction is along the direction of the transmission line, y-direction is vertical to the direction of the transmission line, and z-direction is vertical to the xy-plane and upward

3. Simulation of pulsating wind load

The wind load can be categorised into an average wind load, which produces a static effect on the structure, and a pulsating wind load, which produces a dynamic effect on the structure. These are caused by the average and pulsating wind components in natural wind, respectively.

The pulsating wind speed can be described using a Gaussian stochastic process with an average value of 0. Based on the direction of the varying wind, we can categorise the fluctuating wind speed spectrum into two types: the pulsating wind speed spectrum in the along-wind direction and the pulsating wind speed spectrum in the cross-wind direction. Common along-wind pulsating wind-speed spectra include the Davenport, Solari, and Von Karman spectra. The Davenport spectrum has been extensively utilised and adopted in Chinese standards. In this study, the Davenport spectrum was utilised to express the pulsating wind auto-power spectrum.

$$S_v(f) = 4k\bar{v}_{10}^2 \frac{x^2}{f\left(1+x^2\right)^{4/3}} \quad (1)$$

where $x = 1200f / \bar{v}_{10}$, k is a coefficient related to ground roughness, which is 0.003 for the type A landform; $\bar{v}_{10}$ represents the 10-minute mean wind speed at 10 m above ground level; and f denotes the frequency of the pulsating wind.

The methods utilised for simulating the time history of the pulsating wind speed primarily include wavelet, harmonic superposition, and linear filtering methods. Among them, the autoregressive (AR) model in linear filtering is widely utilised for the time-series analysis of random vibrations owing to its small amount of calculation and fast speed. This study used the AR method to compile a MATLAB program to simulate pulsating wind speed over time. The expression can be written as:

$$v(x,y,z,t) = -\sum_{k=1}^{p} \psi_k v(x,y,z,t-k\Delta t) + N(t) \quad (2)$$

where (x_i, y_i, z_i) (i = 1, 2, ..., m) is the coordinate of point i in space, p is the model order, Δt is the time-step size, Ψ_k is the autoregressive coefficient matrix, and $N(t)$ is an independent random process vector. The initial parameters of the pulsating wind loads are listed in Table 2.

Take N4 tower as an example, the tower was divided into 16 segments, as illustrated in Figure 3 The specific parameters are listed in Table 3. The wind speed–time history and spectrum curves of the tower top and legs are shown in Figures 4 and 5, respectively.

Table 2. Initial parameters of the pulsating wind

Basic wind speed at 10 m height	v_{10} = 32 m/s	Landform category	B
Ground roughness exponent	α = 0.16	Gradient wind height	H_T = 350 m
Correction coefficient of recurrence interval	μ_r = 1.0	Assurance coefficient	μ = 2.2
Wind load arrival time	T_0 = 0.1 s	Total duration	T_{max} = 300 s
Time step	Δt = 0.1 s	Frequency starting point	f_0 = 0.001 Hz
Frequency endpoint	f_{max} = 20 Hz	Frequency increment	Δf = 0.0005 Hz
Number of frequency range segments	N =1 0000	-	-

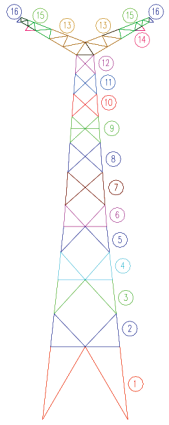

Figure 3. Wind load segmentation of N4 tower

Table 3. Segment parameters of N4 tower

Segment number	Sublevel height [m]	Segment number	Sublevel height [m]
1	13.250	9	101.375
2	31.250	10	109.875
3	42.950	11	117.350
4	53.700	12	124.200
5	63.000	13	132.965
6	71.250	14	136.750
7	80.750	15	138.017
8	91.650	16	139.800

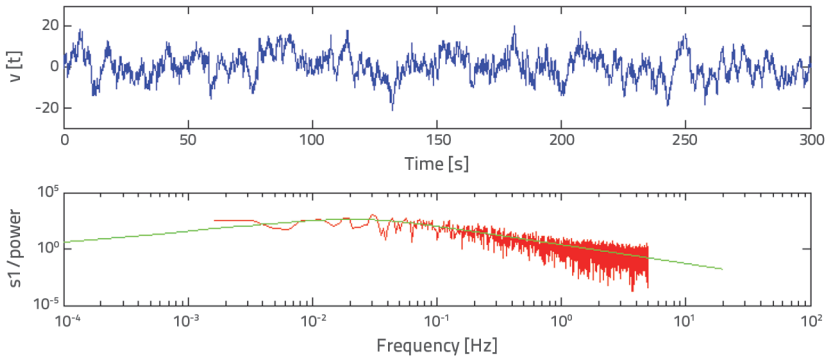

Figure 4. Wind speed–time history curve and self-power spectrum curve at tower top

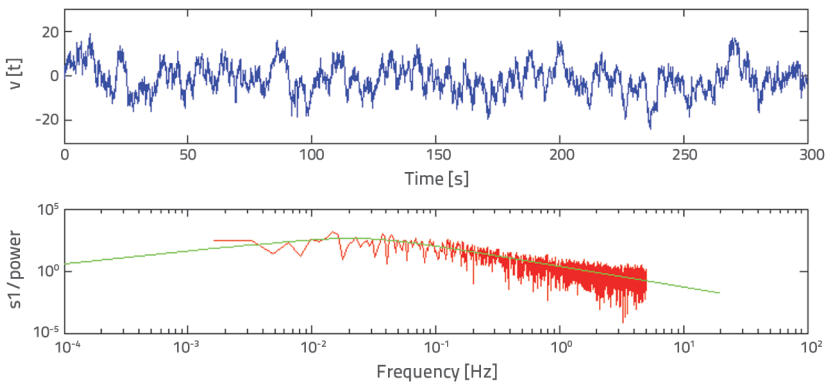

Figure 5. Wind speed–time history curve and self-powered spectrum curve at the tower legs

By comparing the simulated self-power spectrum and target spectrum in Figure 4 and 5, the simulated spectrum aligns well with the target spectrum. The overall mean value of the simulated spectrum closely matches that of the target spectrum, indicating that the values of the various parameters in Table 2 are reasonable and that the simulated spectrum can simulate the real wind field under certain conditions. The wind speed–time history curves for each subsection point were used to analyse the wind vibration response of the transmission towers.

Figure 6 shows the cross-correlation curve of the wind speed between the top of the tower and the cross-arms. Figure 7 shows the cross-correlation curves for the wind speeds at the tops of two adjacent towers.

As seen in Figure 6 and 7, owing to the small distance between the tower top and cross-arm, the wind speeds of the two have a strong correlation, reaching the maximum speed almost simultaneously. However, the distance

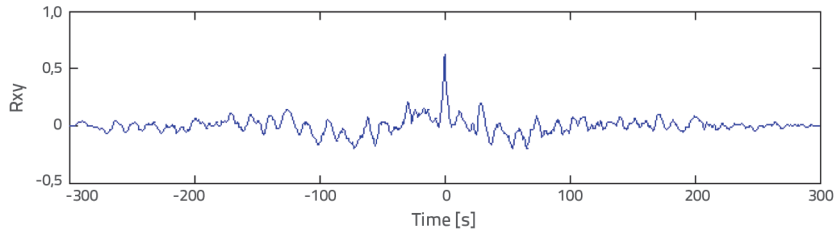

Figure 6. Cross-correlation curve for wind speed between tower top and cross-arm

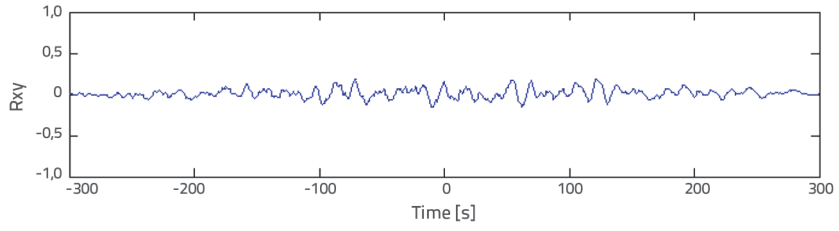

Figure 7. Cross-correlation curve of wind speed at the top of two adjacent towers

between the tops of the two crossing towers was relatively large; therefore, the correlation between the wind speeds was weak.

4. Wind-induced vibration response analysis

4.1. Dynamic characteristics of single tower and tower-line system

A modal analysis was conducted on both the individual tower and the tower-line systems by developing separate finite element models. The first frequencies in three directions of the individual towers are shown in Fig. 8. The first three orders of frequency for the two models are listed in Table 4. According to Table 4, the disparity in the first-order frequency of a single tower between the x- and y-directions was negligible, whereas the first-order torsional natural frequency was approximately 1.65 times higher than that in either the x- or y-direction. Except for the first-order frequency in the y-direction, all the mode frequencies in the tower-line model exhibited lower values than those observed in the single-tower model. The natural

Table 4. First–third order natural frequencies of transmission tower

Vibration mode	Vibration frequency [Hz]		
	Single tower	Tower-line system	
1st order in the x-direction	0.947	in same direction	0.938
		in opposite direction	0.961
2nd order in the x-direction	2.269	in same direction	1.987
		in opposite direction	2.115
3rd order in the x-direction	3.365	in same direction	3.216
		in opposite direction	3.200
1st order in the y-direction	0.955	in same direction	1.009
		in opposite direction	1.000
2nd order in the y-direction	2.353	in same direction	2.236
		in opposite direction	2.281
3rd order in the y-direction	3.743	in same direction	3.672
		in opposite direction	3.669
1st order in the z-direction	1.571	in same direction	1.322
		in opposite direction	1.314
2nd order in the z-direction	3.041	in same direction	2.854
		in opposite direction	2.850
3rd order in the z-direction	5.427	in same direction	5.214
		in opposite direction	5.214

frequency of the tower-line system exhibited a more pronounced decrease in the x direction than in the y direction, indicating that an increase in the mass of the guide and ground wires had a greater impact than the stiffness.

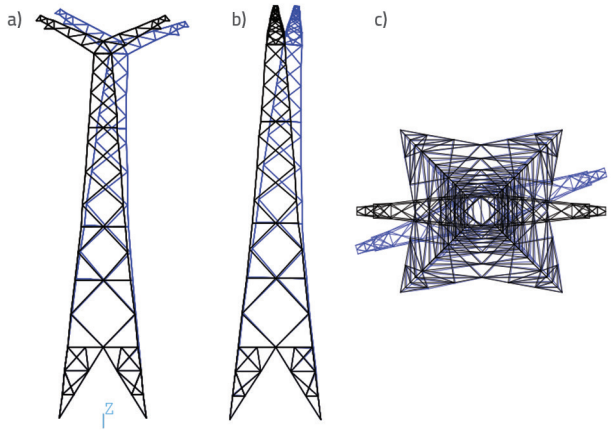

Figure 8. x-, y-, and z-directional first-order formation diagrams: a) 1st order in the x-direction; b) 1st order in the y-direction; c) 1st order in the z-direction

The first-order torsional frequency calculation results of the two models exhibit a significant difference of approximately 16.4%, indicating that the traction of the conductor inhibits torsional vibration in the transmission tower and has a greater constraint effect, more significant than that in the horizontal direction.

4.2. Wind-induced vibration response of single tower

The wind-induced response of the single-tower model was obtained using the finite-element method when the wind angle was 0° (along the direction of the transmission line, same as the y-direction) or 90° (vertical to the direction of the transmission line, same as the x-direction). The wind-induced response time-history curves for the tower top and slope changing point are depicted in Figure 9 and 10, respectively. The axial pressure curves of the main material at the tower leg and the slope-changing point are shown in Figures 11 and 12, respectively.

As shown in Figures 9 and 10, the mean values of the velocity and acceleration at the tower top and changing slope are both zero, and the average displacement is equivalent to the displacement under static loading, indicating that the model load application method is reasonable. The peak displacements at the top and changing

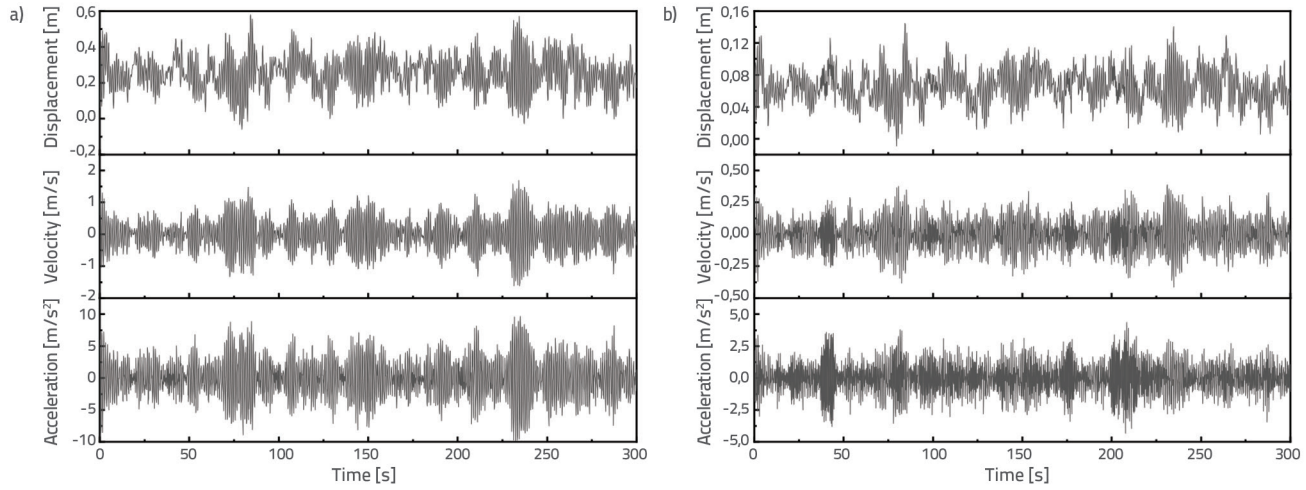

Figure 9. Wind-induced response time history curve of the transmission tower at 0° wind angle: a) Tower top; b) Slope changing point

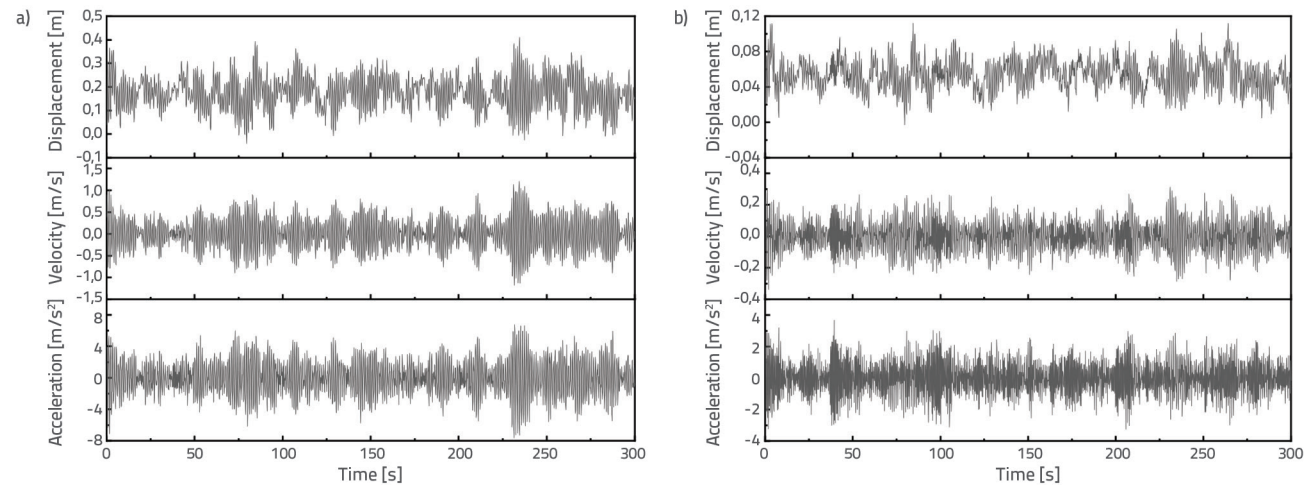

Figure 10. Wind-induced response time history curve of the transmission tower at 90° wind angle: a) Tower top; b) Slope changing point

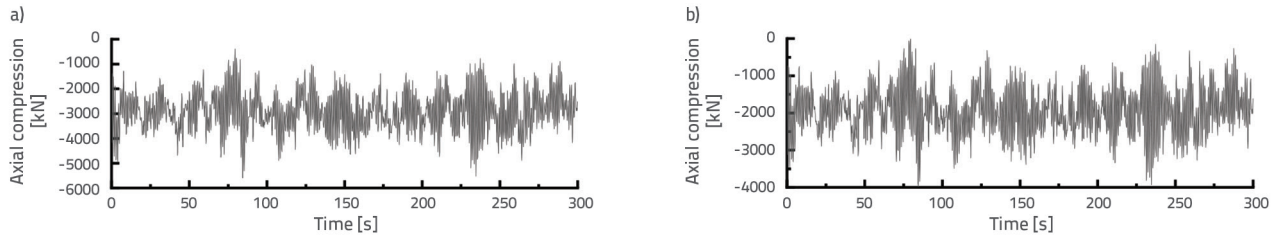

Figure 11. Time history curve of the axial pressure of the main member under a 0° wind angle: a) Tower leg; b) Slope changing point

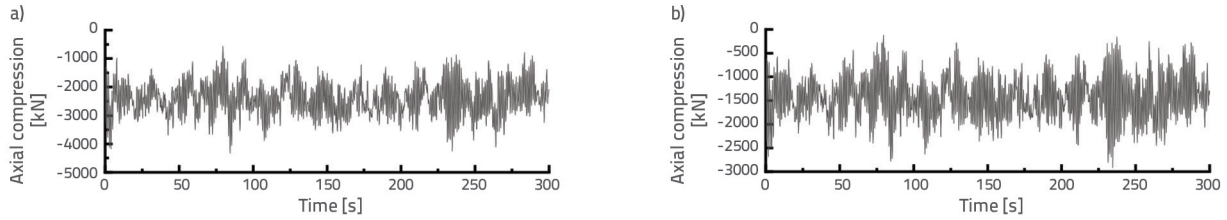

Figure 12. Time history curve of axial pressure of main member at 90° wind angle: a) Tower leg; b) Slope changing point

slope reached 0.580 and 0.151 m, respectively, at a wind angle of 0 °. Similarly, the peak velocities reached 1.693 and 0.415 m/s, respectively, whereas the peak accelerations reached 9.808 m/s^2 and 4.365 m/s^2 respectively. When the wind direction angle was 90°, the displacements at the tower top and tower slope change reached 0.411 and 0.112 m, respectively, the peak velocity reached 1.203 and 0.340 m/s, and the peak acceleration reaches 7.664 m/s^2 and 3.691 m/s^2. The axial forces exerted on the main members at the top and leg of the tower were 3964 N and 5590 kN, respectively, when subjected to a wind direction angle of 0°, as shown in Figures

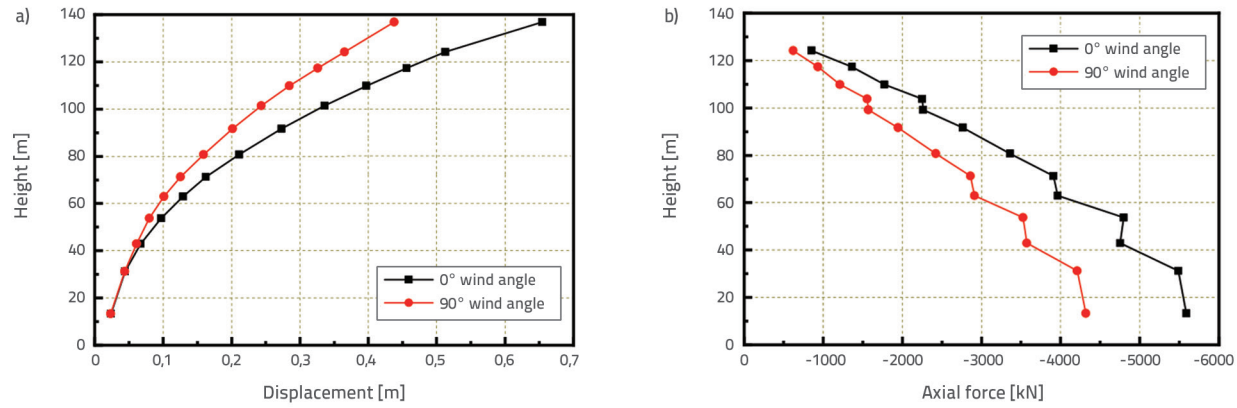

Figure 13. Wind-induced responses of transmission towers at different wind direction angles: a) Tower displacement; b) Axial force of main member of tower

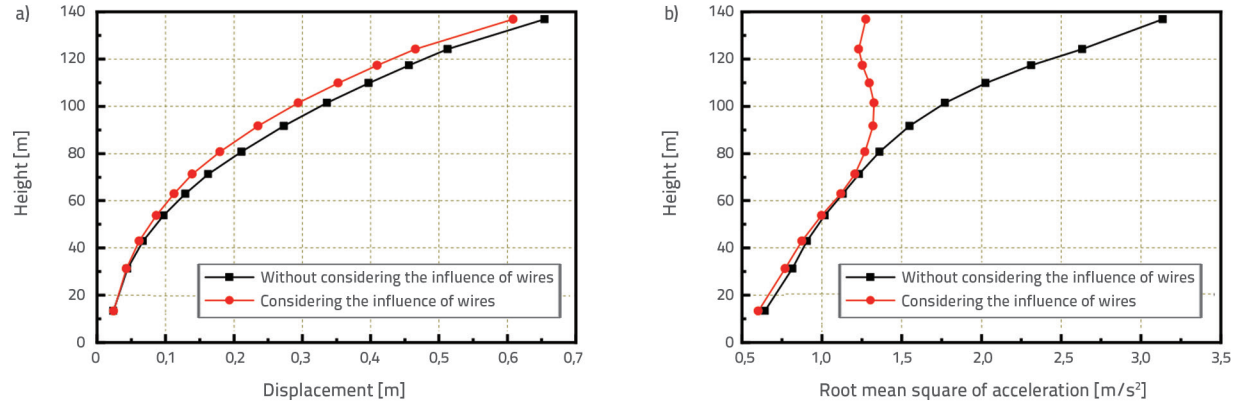

Figure 14. Influence of wire action on wind-induced response of single tower at 0° wind angle: a) Maximum displacement; b) Root mean square of acceleration

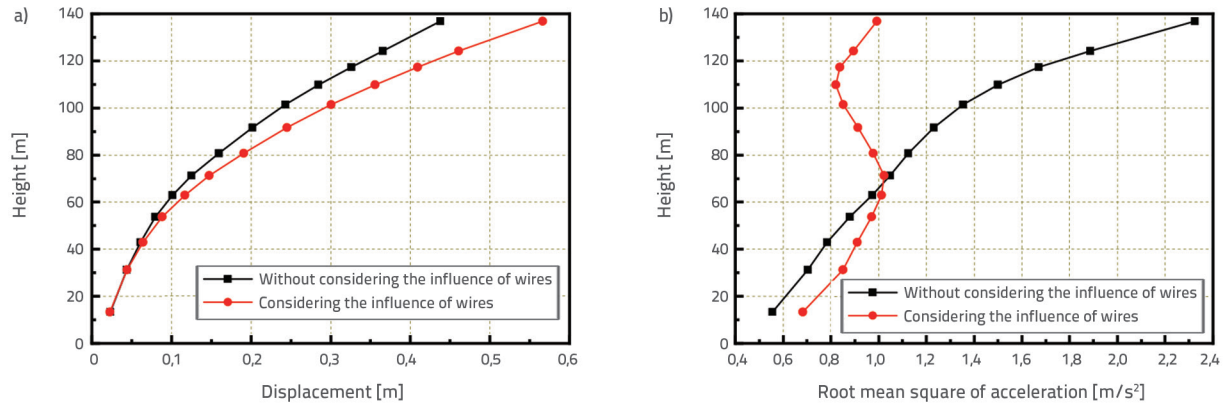

Figure 15. Influence of wire action on wind-induced response of single tower at 90° wind angle: a) Maximum displacement; b) Root mean square of acceleration

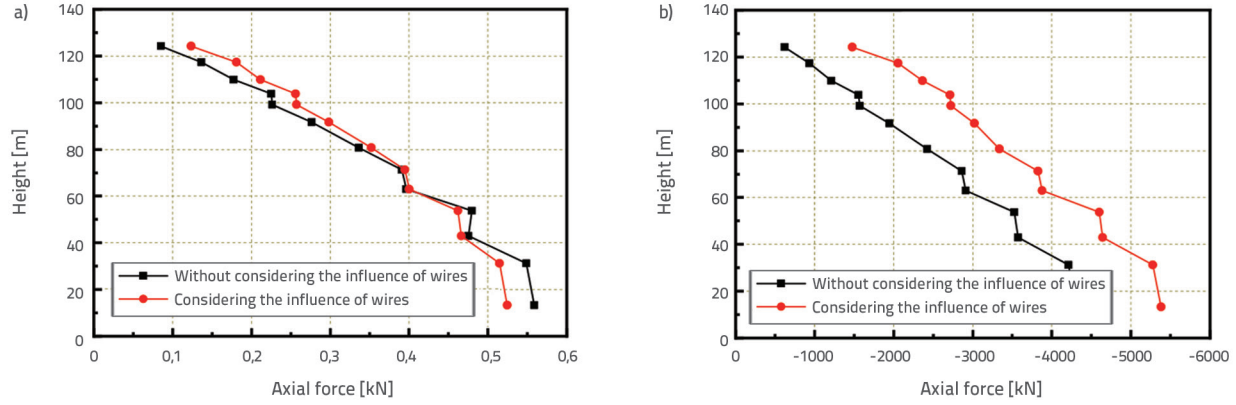

Figure 16. Influence of wire action on axial force of main member of a single tower: a) 0° wind angle; b) 90° wind angle

11 and 12. Similarly, under a wind direction angle of 90 °, these forces were 2914 and 4320 kN for the same locations.

As depicted in Figure 13, the average displacement of the transmission tower gradually increases from the base to the top, with a particularly noticeable increase near the top, owing to a sudden change in the cross-sectional area, leading to a significant increase in the windward surface area. The axial pressure of the main member gradually decreased from the legs to the top. The axial force at the tower leg and the mean displacement at the tower top are approximately 1.3 times and 1.16 times higher, respectively, when the wind direction angle is 0° compared to when it is 90° because, under the condition of a 0° wind direction angle, the front of the cross-arms of the transmission tower is windward.

The impact of the conductor and ground wires on the transmission tower in UHV transmission lines is subject to variations in tower height and span. For small spans, the effects of the conductor and ground wires can be neglected. However, for large-span transmission towers with spans exceeding 1000 m, the impact of wires cannot be overlooked. The MASS21 mass unit in the ANSYS element library was used to apply the mass of the wires to the nodes of the single-tower model, and the single-tower wind-induced responses with and without the additional mass of the wires were calculated.

The results depicted in Figure 14 and 15 demonstrate that when accounting for the influence of the conductor, there was a reduction in the displacement of each segment node of the tower under wind conditions at a direction angle of 0°. Furthermore, the maximum displacement at the top of the tower decreases by approximately 8 %. At a wind angle of 90 °, the maximum displacement of each segment node of the tower increases, and the tower top displacement increases by approximately 22 %. This phenomenon can be attributed to a span exceeding 1000 m, which results in a higher wind load on the conductor when subjected to a 90° wind direction angle, consequently causing increased tower displacement. When considering the impact of the wires, the root mean square acceleration of each node exhibited an increasing trend, followed by a decreasing trend along the height direction of the tower, owing to the decrease in the vibration frequency at the tower top caused by the wire mass, which results in a smaller acceleration variance. Conversely, the areas on the tower body far from the wire hanging points were less affected by the wire mass, and the root mean square of the acceleration was larger than that at the top of the tower.

The function of the conducting wire did not affect the variation trend of the axial force along the tower height, as shown in Fig. 16. Under the influence of a 0° wind, the wire action has a small impact on the axial force values of each node bar. When subjected to a 90° wind, the action of the conductor wire significantly increased the axial force at each node. Specifically, the axial force of the tower leg node member increased by approximately 25 %, whereas the axial force at

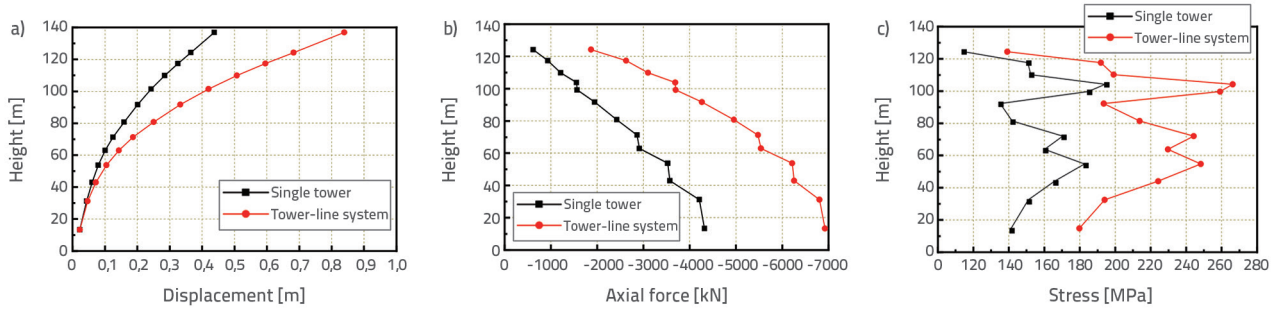

Figure 17. Comparison of wind vibration responses between single-tower and tower-line systems: a) Maximum displacement; b) Axial force of main material; c) Stress

the tower top node increased by approximately 138 %. The influence of the wires on the transmission tower increased from the bottom to the apex.

4.3. Wind-induced vibration response of tower-line system

Considering the extensive span of the transmission tower-line system, the conductor wire experiences the highest wind pressure when exposed to a 90° wind direction. Therefore, analysing the wind-induced response exclusively when the wind direction angle is 90° is imperative. Taking the N4 crossing tower as an example, the results are shown in Fig. 17.

The results depicted in Figure 17 demonstrate that the tower-line system exhibits a maximum displacement of 0.839 m under a 90° wind direction angle, which occurs in the tower top segment and is approximately 1.92 times the maximum displacement of a single tower. The maximum axial pressure exerted on the tower-line system is 6924 kN, which occurs in the tower leg segment and is approximately 1.60 times the maximum axial pressure of a single tower. The variation trend of the stress of a single tower along the tower height was consistent with that of the tower-line system. The maximum stress value of a single tower was 195.3 MPa, whereas that of the tower-line system reaches 267.8 MPa, representing an increase of approximately 37 % compared to the stress in a single tower. The interaction between the tower and transmission line significantly influences the displacement and stress of the tower.

5. Conclusion

ANSYS finite element models of a single tower and a tower-line system consisting of five towers and four spans of transmission lines were established in this study. The dynamic characteristics and wind-induced responses of a single tower and tower line system under a pulsating wind load were obtained using numerical simulations. The impact of tower-line coupling on the wind-induced responses of transmission towers was investigated. By comparing the finite element simulation results under different working conditions, the following conclusions were drawn:

The conductor and ground wire exhibited high flexibility and low stiffness, leading to a lower vibration frequency of the tower-wire system than that of an individual tower. Notably, the torsional natural frequency decreased most significantly, indicating that the influence of the conductor mass was greater than that of the conductor stiffness; this effect was stronger in the torsion direction. The axial force of the main material and the displacement of a single tower in the 0° wind direction angle condition were greater than those in the 90° wind direction angle condition, a more unfavourable state.

The wind-induced response of the tower-line system was significantly amplified owing to the tower-line coupling effect. The maximum displacement of the tower-line system was approximately 1.92 times greater than that of a single tower, whereas the maximum axial pressure on its main material was approximately 1.60 times higher than that on a single tower. Furthermore, the tower-line system was subjected to approximately 1.37 times the stress of a single tower. Therefore, considering the influence of tower-line coupling during the design phase of transmission towers with extensive spans is imperative. If deemed necessary, damping devices may be installed to limit wind-induced vibrations effectively.

Acknowledgements

This study was supported by the Science and Technology Project of the State Grid Corporation of China (Project No. 5108-202218280A-2-318-XG).

REFERENCES

[1] Zhang, Z.Q., Li, H.N., Li, S.F., Ren, Z.D., Zhang, P., Li, N.: Disaster analysis and safety assessment on transmission tower-line system: an overview, China Civil Engineering Journal, 49 (2016) 12, pp. 75-88, https://doi.org/10.15951/ j.tmgcxb.2016.12.009.

[2] Ozono, S., Maeda, J.: In-plane dynamic interaction between a tower and conductors at lower frequencies, Engineering Structures, 14 (1992) 4, pp. 210-216.

[3] Albermani, F.G.A., Kitipornchai, S.: Numerical simulation of structural behaviour of transmission towers, Thin-Walled Structures, 41 (2003), pp. 167-177.

[4] Yasui H., Marukawa H., Momomura Y., Ohkuma T. Analytical study on wind-induced vibration of power transmission towers. Journal of Wind Engineering and Industrial Aerodynamics, 83 (1999), pp. 431-441.

[5] Geng, Z.W., Su, W.W., Yu, F.R., Qian, J.: Analysis of wind vibration response of high-voltage transmission tower based on ANSYS, Electrical Measurement & Instrumentation, 60 (2023) 02, pp. 84-90, https://doi.org/10.19753/j.issn1001-1390.2023.02.012.

[6] Guo, Y., Sun, B.N., Ye, Y.: Time-domain analysis on wind-induced dynamic response of long-span power transmission line systems. China Civil Engineering Journal, 39 (2006) 12, pp. 12-17.

[7] Yu, C.Y., Zhang, J.R.: Analysis of dynamic characteristics and wind-induced vibration response of transmission line systems, Journal of Southeast University (Natural Science Edition), 49 (2019) 01, pp. 116-124.

[8] Zhang, Q., Ye, Z., Cai, J.G., Yu, L., Feng, J.: Wind-induced response of UHV long cantilever transmission tower and tower-line coupled system, Journal of Southeast University (Natural Science Edition), 49 (2019) 01, pp. 1-8.

[9] Zhang, Q., Ye, Z., Cai, J.G., Yu, L., Feng, J.: Wind-induced torsional response of UHV long cantilever transmission tower, Journal of Central South University (Science and Technology), 51 (2020) 04, pp. 1108-1115.

[10] Zhang, Q., Fu, X., Ren, L., Jia, Z.G.: Modal parameters of a transmission tower considering the coupling effects between the tower and lines, Engineering Structures, 220 (2020), pp. 110947, https://doi.org/10.1016/ j.engstruct.2020.110947.

[11] Zhu, Y. X., Zhang, R. Y., Cao, M. G., Tu, F., Wang, Y., Zheng, C.: Wind-induced vibration response and coefficient of large crossing transmission tower line system between islands, High Voltage Apparatus, 58 (2022) 01, pp.111-121, https://doi.org/10.13296/j.1001-1609. hva.2022.01.015.

[12] Wang, W.M., Sun, Z.D., Zeng Y.J., Tian, L.: Wind Tunnel Test on Wind-Induced Vibration Response of Long-span transmission tower-line system. Industrial Construction, 47 (2017) 05, pp. 79-84+95, https://doi.org/10.13204/ j.gyjz201705016.

[13] Lou, W.J., Jiang Y., Jin X.H., Wang, Z.H., Xia, L., Shen, G.H.: Wind t-unnel test research on wind-induced vibration characteristics of angle steel tower in typhoon field, Journal of Vi-bration Engineering, 26 (2013) 02, pp. 207-213, https://doi.org/10.16385/j.cnki.issn.1004-4523.2013.02.018.

[14] Deng, H.Z., Duan, C.Y., Xu, H.J.: Wind tunnel tests on an aeroelastic model of a transmission tower-line system under normal wind field and typhoon wind field, Journal of Vibration and Shock, 37 (2018) 08, pp. 257-262, https://doi.org/10.13465/j.cnki.jvs.2018.08.038.

[15] Yang, Z.Y., Song, X.Q., Deng, H.Z.: Frequency domain analysis of wind-induced response of ±1100 kV ultra high voltage (UHV) transmission tower, Journal of Central South University (Science and Technology), 51 (2020) 08, pp. 2121-2131.